Post-translational modifications drive protein stability to control the dynamic beer brewing proteome

Edward D. Kerr[1] and Benjamin L. Schulz[1,2*].

[1] School of Chemistry and Molecular Biosciences, The University of Queensland, St Lucia 4072, Queensland, Australia.
[2] Centre for Biopharmaceutical Innovation, Australian Institute of Bioengineering and Nanotechnology, The University of Queensland, St Lucia 4072, Queensland, Australia.

[*] To whom correspondence should be addressed: Benjamin L. Schulz, b.schulz@uq.edu.au, +61 7 3365 4875.

Abstract

Mashing is a key step in beer brewing in which starch and proteins are solubilized from malted barley in a hot water extraction and digested to oligomaltose and free amino nitrogen. We used SWATH-MS to measure the abundance and site-specific modifications of proteins throughout a small-scale pale ale mash. Proteins extracted from the malt at low mash temperatures decreased precipitously in abundance at higher temperatures due to temperature-induced unfolding and aggregation. Correlation analysis of temperature-dependent abundance showed that sequence and structure were the main features that controlled protein abundance profiles. Partial proteolysis by barley proteases was common early in the mash. The resulting proteolytically clipped proteins were particularly temperature sensitive and were preferentially lost at high mash temperatures, while intact proteins remained soluble. The beer brewing proteome is therefore driven by the interplay between protein solubilisation and proteolysis, which are in turn determined by barley variety, growth conditions, and brewing process parameters.

Introduction

Beer brewing is a well-established industrial process comprising a series of connected bioprocesses (Fig. 1A). Harvested barley seeds are turned into malt through a process called malting, which involves controlled germination and drying (1, 2). Mashing then extracts soluble components from the malt and allows enzymes to degrade starch into small fermentable sugars and proteins into free amino nitrogen (FAN) (1). The soluble product of mashing is called wort, which is boiled with hops to sterilize, introduce bitterness, remove volatile off-flavours, and stop enzymatic activity (1, 3). Fermentation is the next stage of the brewing process, in which yeast ferments sugars to ethanol, producing beer. This beer can then be optionally filtered to create "bright beer", or left unfiltered, further aged or not, carbonated, and packaged.

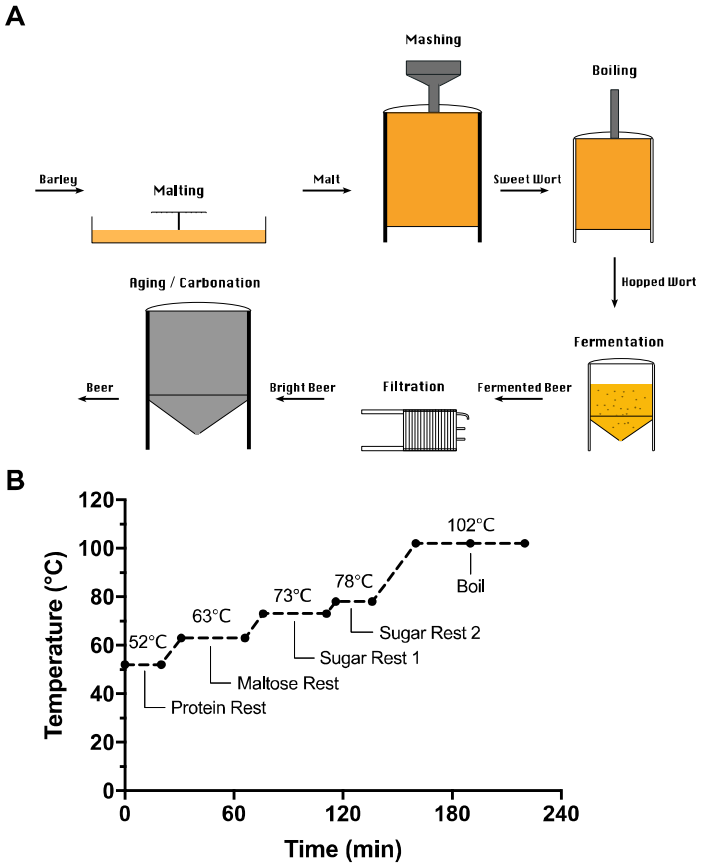

Figure 1. Overview of the brewing process. (**A**) Overview of the brewing process from malting to beer. (**B**) Mashing program used in this study.

While it is appreciated that the mash and boil entail complex biochemistry, the details of aspects of these processes are poorly understood. Proteomic studies have identified

many proteins in wort and in beer, highlighting that some proteins can survive proteolysis in the mash and heating during malting and boiling (4-10). Studies using two-dimensional gel electrophoresis (2-DE) and mass spectrometry identified these heat-stable proteins as cysteine-rich plant defence proteins, α-amylase/trypsin inhibitors, and non-specific lipid transfer proteins (4, 5). More recent studies have shown that the wort and beer proteome is highly complex, and contains hundreds of unique proteins from barley and yeast (6-10). Complex post-translational modifications including proteolysis, oxidation, and glycation are also present on proteins in wort and beer (8, 11, 12). While these studies demonstrate the complexity of the wort and beer proteomes, precisely when during the brewing process protein modification occurs and how the wort proteome changes during the mash remain unexplored.

Proteins are extracted from malt during the mash and are subsequently denatured, aggregated, and precipitated at higher temperatures in the mash or boil (3). However, the proteome-wide extent of temperature-dependent protein aggregation during mashing has not been studied. Proteome thermal profiling has been performed of other complex systems including studying proteome-wide drug-protein interactions in mammalian cells (13-16). This approach measures the thermal stability of every detectable protein in a proteome by LC-MS quantification of the fraction of each protein that is soluble after incubation at various temperatures. The proteome thermal profiling workflow mimics the temperature ramp used in typical beer mashing and boiling, and by analogy suggests that the dynamic wort proteome is balanced by competing processes including protein solubilisation, modification, and aggregation.

In this study, we used Sequential Window Acquisition of All THeoretical Mass Spectra (SWATH-MS) to address the complexity of the dynamics of protein abundance and modification during beer brewing. We uncover an incredible complexity of protein modifications and show that an interplay of partial proteolysis and temperature-dependent protein unfolding drive the proteome of wort and beer.

Methods

Experimental design and statistical rationale

A small-scale mash was performed using a Braumeister (Speidel) with 23 L of water and 5 kg of milled Vienna pale ale malt (Brewer's Choice, Brisbane) with a multi-step mash (Table S1 and Fig. 1B). Samples were taken at the start and end of each stage, and after 30 min of boil. Samples were clarified by centrifugation at 18,000 rcf at room temperature for 1 min immediately after sampling, and the supernatants stored at -20˚C. Samples were taken from independent triplicate mashes using malt from the same batch. Proteins from 10 µL of each sample were precipitated by addition of 100 µL 1:1 methanol/acetone, incubation at -20˚C for 16 h, and centrifugation at 18,000 rcf at room temperature for 10 min. Proteins were resuspended in 100 µL 100 mM ammonium acetate and 10 mM dithiothreitol with 0.5 µg trypsin (Proteomics grade, Sigma) and digested at 37 °C with shaking for 16 h. Trypsin was added at equal amounts to all samples to allow normalisation of relative protein abundance. SWATH-MS was implemented as described below using triplicates to reduce retention time variation and improve data quality.

SWATH-MS

Peptides were desalted with C18 ZipTips (Millipore) and measured by LC-ESI-MS/MS using a Prominence nanoLC system (Shimadzu) and TripleTof 5600 mass spectrometer with a Nanospray III interface (SCIEX) essentially as previously described (17). Approximately 1 µg or 0.2 µg desalted peptides were injected for data dependent acquisition (DDA) or data independent acquisition (DIA), respectively. Peptides were separated on a VYDAC EVEREST reversed-phase C18 HPLC column (300 Å pore size, 5 µm particle size, 150 µm i.d. x 150 mm) at a flow rate of 1 µl/min) with a linear gradient of 10-60% buffer B over 14 min, with buffer A (1% acetonitrile and 0.1% formic acid) and buffer B (80% acetonitrile and 0.1% formic acid), for a total run time of 24 min per sample. LC parameters were identical for DDA and DIA, and DDA and DIA MS parameters were set as previously described (18).

Data analysis

Peptides and proteins were identified using ProteinPilot 5.1 (SCIEX), searching against all eukaryotic proteins in UniProtKB, with settings: sample type, identification; cysteine alkylation, none; instrument, TripleTof 5600; species, none; ID focus, biological modifications; enzyme, trypsin; search effort, thorough ID. The abundance of peptide fragments, peptides, and proteins was determined using PeakView 2.1 (SCIEX), with settings: shared peptides, allowed; peptide confidence threshold, 99%; false discovery rate, 1%; XIC extraction window, 6 min; XIC width, 75 ppm. The mass spectrometry proteomics data have been deposited to the ProteomeXchange Consortium via the PRIDE partner repository with the dataset identifier PXD010013(19). For protein-centric analyses, protein abundances were normalised to trypsin. For analysis of peptide modifications, the abundance of each variant form of a peptide was normalised to the summed abundance for all detected forms of that peptide.

Proteins were clustered based on correlation profiling of their abundance throughout the mash. We defined a measure of distance between pairs of proteins based on how different their abundances were at each time point. The distance between protein *a* and protein *b* was given by: $d_{a,b} = \sum_{t=0}^{n} |A_{a,t} - A_{b,t}|$, where $A_{a,t}$ is the normalised abundance of protein *a* at time point *t*. The difference between every pair of proteins across the entire temperature profile was then calculated by summing the distance across all time points for each protein. Proteins with similar stability profiles were clustered using Cluster 3.0 (20), implementing a hierarchical, uncentered correlation, and complete linkage on both x and y. Clustered data were represented as a heat map using Plotly (1.12.2). Physicochemical properties of proteins including amino acid length, molecular weight, pI, aliphatic index, charge at pH 7, charge at pH 5, hydrophobicity, and amino acid composition was calculated using Peptides 2.2 (21). GO term enrichment was determined using GOstats (22) in R using a significance threshold of P = 0.05.

Results

Enzymes degrade starch and proteins during the mash to produce oligomaltose sugars and FAN, while boiling the wort halts enzyme activity by denaturing proteins. We used a step mash with a protein rest (period of stationary temperature) at 52°C for 20 min, maltose rest at 63°C for 35 min, sugar rest 1 at 73°C for 35 min, sugar rest 2 at 78°C for 20 min, and finally the boil at 102°C for 60 min (Fig. 1B). This temperature ramp allowed detailed analysis of the temperature dependent changes in the wort proteome during the mash and boil. Liquor was sampled at the start and end of each rest and after 30 min of the boil, clarified by centrifugation, precipitated, digested by trypsin, desalted, and analysed by SWATH-MS.

We identified peptides and proteins in the samples using DDA LC-MS/MS detection and ProteinPilot identification. Protein identification, quantification, and raw mass spectrometry data are available via the PRIDE partner repository with the dataset identifier PXD010013. We identified a total of 87 unique proteins. As we searched the entire UniProt database some non-barley proteins were identified, and these likely correspond to unannotated proteins in the barley proteome. Of the proteins identified, 7 were involved in starch degradation, 21 were defence proteins, 7 were nutrient reservoirs, 12 were amylase/protease inhibitor proteins, and the majority of the remainder were house-keeping proteins.

Global proteomic changes during mashing

After identifying peptides and proteins, we measured the abundance of each protein in each sample using SWATH-MS and PeakView, normalising protein abundance to trypsin self-digest peptides. This allowed us to determine changes in protein abundance during the mash and boil, and thereby measure protein-specific extraction, solubilisation, aggregation, and precipitation of proteins during mashing. Our data showed that the abundance of most proteins increased during the maltose rest (63°C) and sugar rest 1 (73°C), and then decreased substantially during sugar rest 2 (78°C) and into the boil (102°C) (Fig. 2A). This is consistent with efficient extraction of proteins from the grain at lower temperatures, followed by temperature-dependent unfolding, aggregation, and precipitation at higher temperatures.

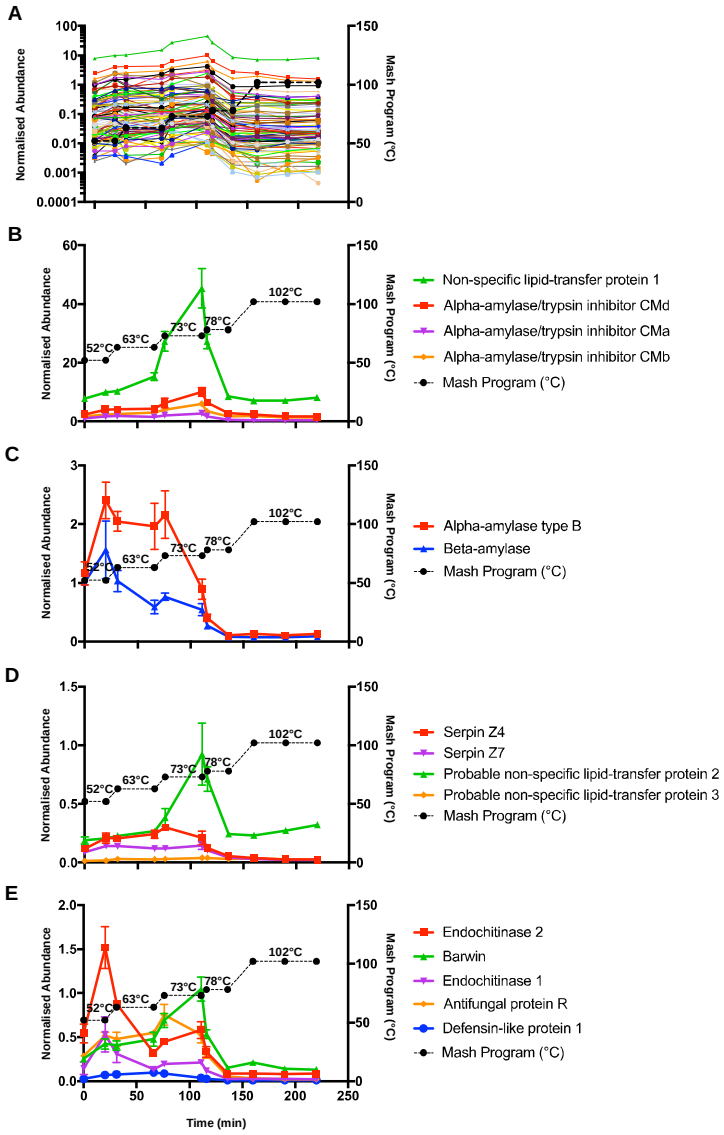

Figure 2. Dynamics of protein abundance during the mash and boil. (**A**) Log-scale abundance of all 87 identified and measured proteins. Error bars and protein names not shown for clarity. Each protein is represented by a different colour. (**B**) Abundance of the four most abundant proteins: α-amylase/trypsin inhibitor CMd (IAAD), non-specific lipid-transfer protein 1 (NLTP1), α-amylase/trypsin inhibitor CMa (IAAA), and α-amylase/trypsin inhibitor CMb (IAAB). (**C**) Abundance of α-amylase type B (AMY2) and β-amylase (AMYB). (**D**) Abundance of beer foam formation and stability proteins: Serpin Z4, Probable non-specific lipid-transfer protein (NLTP2), Serpin Z7, and Probable non-specific lipid-transfer protein (NLTP3). (**E**) Abundance of selected defence proteins: endochitinase 2 (CHI2), barwin (BARW), endochitinase 1 (CHI1), antifungal protein R (THHR), and

defensin-like protein 1 (DEF1). A – E: Abundance (a.u; arbitrary units) of each protein normalised to trypsin. Values show mean, n=3. Error bars show SD. Mash temperature profile is shown on right Y-axis.

To understand how the relative abundance of proteins changed during the mash, and what characteristics determined the stability of a protein during the mash and boil, we visualised the relative abundance of classes of proteins that are of particular importance to barley and beer quality: the most abundant proteins, α and β-amylase, beer foam forming or associated proteins, and defence proteins. NLTP1 (non-specific lipid-transfer protein 1) was the most abundant protein as measured by MS peptide signal throughout the mash, followed by IAAD, IAAA, and IAAB (Fig. 2B). The abundance of these proteins increased until the end of the first sugar rest (73°C), after which their abundance quickly declined by the end of the second sugar rest (78°C).

α- and β-amylase are critical for the hydrolysis of starch into fermentable sugars by cleaving starch at internal α(1, 4) linkages and at non-reducing ends, respectively (1, 3, 23). The activities of these enzymes *in situ* during the mash have been reported to peak at 63˚C for both α and β-amylase, and decline above 70˚C for α-amylase and at 65˚C for β-amylase (24, 25). Our proteomic analysis showed that α- and β-amylase initially had similar levels of abundance in the mash (Fig. 2C). The abundance of α-amylase increased during the protein rest (52°C) and was stable until the first sugar rest (73°C) where it slowly declined to be essentially absent at the end of the second sugar rest (78˚C). β-amylase followed a similar trajectory but at consistently lower abundance. The temporal abundance of these proteins we observed here is therefore consistent with the temperature-dependent enzyme activities (24, 25), consistent with soluble enzyme abundance driving overall amylase activity in wort.

We detected several proteins which have been reported to play roles in beer foam formation and stability: non-specific lipid-transfer proteins 1 – 3 (NLTPs), Serpin Z4, and Serpin Z7 (Fig. 2B, D). Lipid-transfer proteins (LTPs) and serpin proteins are reported to be positively associated with beer foam formation and stability (26-28). LTPs all increased in abundance until the end of the maltose rest (63°C) then decreased once temperature rose above 63°C (Fig. 2B, D). Serpin proteins increased

until the maltose rest (63°C), then decreased in abundance (Fig. 2D). Interestingly, a substantial fraction of NLTP1 and NLTP2 were still abundant throughout the boil and into the final beer (Fig. 2B, D).

Anti-fungal defence proteins were abundant throughout the mash (Fig. 2E), consistent with previous proteomic studies of barley and beer (4-6, 29, 30). We therefore examined how the abundance of key defence proteins changed during the mash (Fig. 2E). These proteins were all efficiently extracted at low temperatures, and then showed diverse abundance profiles throughout the mash. At the beginning of the mash, 26 kDa endochitinase 2 (CHI2) was the most abundant defence protein, but its abundance decreased at the maltose rest (63°C). 26 kDa endochitinase 1 (CHI1) followed a similar trend, but at a consistently lower abundance (Fig. 2E). While CHI1 and CHI2 abundance decreased during the first sugar rest (73˚C), Barwin (BARW) and Antifungal Protein R (THHR) increased during this stage. The abundance of BARW and THHR then decreased until the end of the second sugar rest (78°C). Defensin-like protein 1 (DEF1) had a low abundance throughout the mash compared to other defence proteins but increased during the maltose (63°C) and first sugar rest (73°C). Defence proteins were generally amongst the most stable proteins, as they were present at high abundance until the first sugar rest (73˚C), and were still present at moderate levels at the end of the boil.

Correlation profiling of protein abundance throughout the mash

To further understand the dynamics of protein abundance throughout the mash we performed protein correlation profiling. We performed a pairwise comparison between every protein at every period of the mash and then calculated a distance matrix between each pair of proteins. This distance matrix allowed the comparison of abundance profiles between proteins. We then performed a cluster alignment to group proteins with similar abundance profiles (Fig. 3A). This analysis identified four clusters of proteins that were primarily distinguished by the temperature at which the proteins reached maximum abundance (Fig. 3A, B). The presence of four distinct clusters of temperature-dependent abundance suggested that there were sequence, physical, or biochemical features shared between proteins in each cluster. To discover these features, we calculated a variety of theoretical physicochemical properties for each protein. Proteins in cluster three were significantly larger than proteins in

clusters one and two, as measured by amino acid length or molecular weight (Fig. 3C), and were enriched in aromatic amino acids (Fig. 3D). Cluster three also had the lowest temperature of maximum protein abundance of the four clusters (Fig. 3B), consistent with larger and more hydrophobic proteins being more susceptible to temperature-dependent unfolding and aggregation (8). Cluster one had the highest temperature of maximum abundance (Fig. 3B) and was enriched in cysteines (Fig. 3C), consistent with abundant disulfide bonds increasing protein stability.

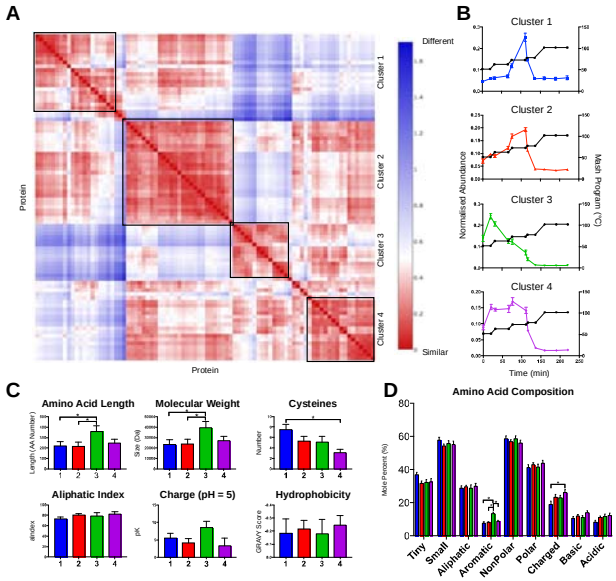

Figure 2. Correlation profiling of protein abundance throughout the mash. (A) Proteins clustered using Cluster 3.0, and heat mapped. Colour represents difference in abundance profiles of each pair of proteins: red, similar; blue, different. **(B)** cluster 1 – 4. **(C)** protein length, molecular weight, number of cysteines, aliphatic index, protein net charge at pH = 5, and hydrophobicity. Values show mean of proteins within a cluster, error bars show SEM. **(D)** Amino acid composition of proteins in each cluster. * indicate significant ($p < 0.05$) differences between groups.

The temperature-dependent abundance profiles of homologous proteins tended to be similar (Fig. 2), and each cluster of proteins with correlated abundance profiles had a unique physicochemical profile (Fig. 3). Together, this suggested that each cluster (Fig. 3A, B) consisted of homologous or related proteins. We tested this using GO term enrichment analysis on the four clusters to identify terms and pathways

associated with proteins belonging to each cluster. Each cluster was significantly enriched in at least one GO term (Table S2). Cluster one was associated with lipid binding, due to enrichment of Lipid Transfer Proteins homologous to the abundant NLTP1. Cluster two was enriched in peptidase inhibition, associated with Chloroform/Methanol soluble proteins homologous to IAAA. Cluster three was enriched with hydrolase activity from amylases and chitinases. Lastly, cluster four was enriched in the generic GO term catalytic activity, from several functionally diverse cytoplasmic proteins. In summary, this showed that proteins in clusters one to three were enriched in homologous proteins likely to share sequence similarities, consistent with their correlated temperature-dependent abundance profiles. Together, these analyses showed that protein sequence and structural characteristics were the primary factors that controlled temperature dependent protein abundance profiles during the mash.

Protein modification drives stability

While all proteins decreased in abundance at higher temperatures, there were many proteins for which a substantial fraction survived the boil (e.g. NLTP1, NLTP2, BARW, CHI1; Fig. 2B, D, E). These proteins would potentially remain in the final beer, and have indeed been detected in beer (6-8, 31). This clear distinction in temperature sensitivity between pools of the same protein suggested that covalent modifications may be driving diversity of protein structure and behaviour. To understand what allowed this small fraction of proteins to survive the boil we investigated proteome-wide changes in the abundance of site-specific modifications during the mash and boil.

Protein modifications including oxidation, glycation, and proteolytic cleavage are common in brewing, and impact beer product qualityo(8, 12, 32-35). We identified many sites with these modifications in proteins in wort. The thermal stability of proteins and their ability to survive the boil intact could be altered by these modifications. To test this, we investigated the dynamics of site-specific proteolysis and chemical modification in proteins during the mash and boil.

The barley proteases responsible for proteolysis during mashing are active at lower temperatures, where they cleave proteins during the protein rest (52°C) and add FAN

to the wort (1, 3, 23, 33, 36, 37). As well as creating FAN, proteolysis influences protein stability. To monitor proteolysis during the mash we first identified non- or semi-tryptic peptides in the wort throughout the mash and boil. Not unexpectedly, proteolysis was a very common modification of proteins identified throughout the mash, with 59% of peptides detected as non- or semi-tryptic peptides. Inspection of homology models of protein structures showed that all sites of proteolysis we detected could be mapped to the surface of the substrate protein (Fig. 4, 5, Fig. S1 – S3). This is consistent with proteolytic enzymes acting on otherwise intact and folded proteins in the grain or wort, and proteolysis being limited to a few events for each individual protein.

Accurate determination of the effect of proteolysis on protein stability required high peptide coverage, and so we examined proteolysis in proteins that had many peptides identified: BARW, NLTP1, α-amylase/trypsin inhibitor CMa (IAAA), α-amylase/trypsin inhibitor CMb (IAAB), α-amylase/trypsin inhibitor CMd (IAAD), and α-amylase (AMY2). We grouped semi-tryptic derivatives of the same full tryptic peptide, and normalised their abundances to the sum of their total intensities at each time point during the mash and boil. For all peptides analysed, semi-tryptic derivatives increased in abundance and were dominant during the protein rest (52°C) and the beginning of the maltose rest (63°C) (Fig. 4, 5, Fig. S1–S3), consistent with abundant protease activity at these temperatures (1, 3, 23, 33, 36, 37). However, when the mash temperature rose above 63°C, these semi-tryptic peptides decreased in abundance relative to the full tryptic form (Fig. 4, 5, and Fig. S1 – S3). Typically, this occurred at the same temperature at which the overall abundance of that protein decreased in the wort (Fig. 2A). We interpreted this effect as corresponding to proteolytically clipped forms of proteins unfolding and aggregating at temperatures at which the intact form of the protein remained stable. For example, most semi-tryptic derivatives of K-M_{36}KPCLTYVQGGPGPSGECCNGVR_{58}-D and K-C_{99}NVNVPYTISPDIDCSR_{115}-I from NLTP1 were more abundant at 52°C than the full tryptic form, and above 73°C these cleaved forms drastically decreased (Fig. 4C, D, E). This pattern was typical of most sites of proteolysis that could be confidently examined (Fig. 4, 5, and Fig. S1 – S3).

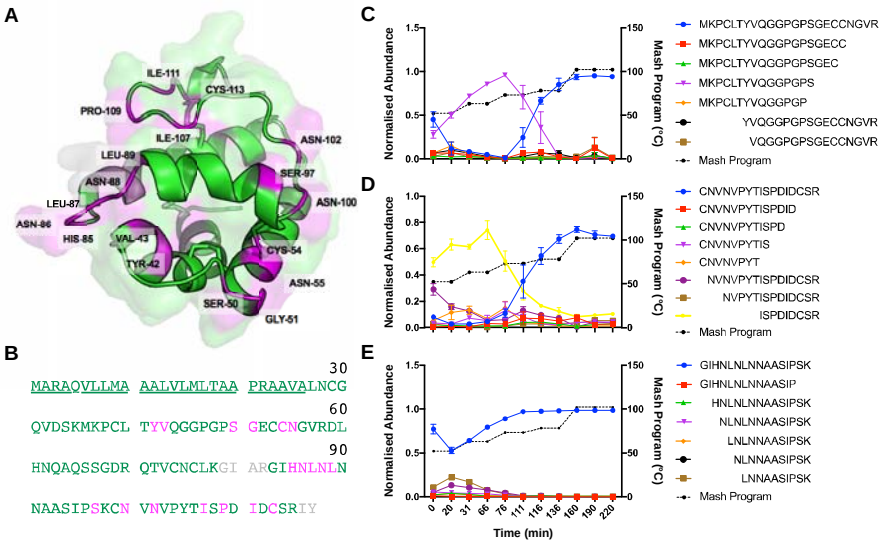

Figure 4. Proteolysis during the mash lowers the stability of NLTP1. (A) Cartoon of the X-ray crystal structure of NTLP1 (1MID). Green, peptides identified by MS; grey, unidentified peptides; magenta and labelled, amino acid after a proteolytic cleavage event. **(B)** NLTP1 protein sequence with the same colour scheme as (A). Underlined, not present in structure. Normalised abundance (a.u; arbitrary units) of full- and semi-tryptic peptides corresponding to **(C)** K-M_{36}KPCLTYVQGGPGPSGECCNGVR$_{58}$-D, **(D)** K-C_{99}NVNVPYTISPDIDCSR$_{115}$-I, and **(E)** R-G_{83}IHNLNLNNAASIPSK$_{98}$-C. Values show mean, n=3. Error bars show SD. Mash temperature profile is shown on the right Y-axis. Mash program is shown in black dotted lines; points indicate when samples were taken.

Interestingly, a few select proteolytic cleavage events did not affect temperature-dependent protein abundance (Fig. 5D, S1D, and S2E). In IAAA, two semi-tryptic derivatives of K-V_{122}LVTPGQCNVLTVHNAPYCLGLDI$_{145}$ (C-terminus) (with cleavage between H_{135}-N_{136} or between D_{144}-I_{145}) were stable at higher temperatures and were even more abundant than the full tryptic peptide (Fig. 5). We inspected a model of the structure of IAAA to provide insight into why proteolysis at these sites might be tolerated. Disulfide bonds between C_{140} and C_{87}, and between C_{129} and C_{75}, likely lock the local protein fold in place to provide stability even after cleavage at H_{135}-N_{136}. In contrast, the C-terminal 2 amino acid residues in the model of IAAA are not defined, suggesting this region is structurally flexible. Proteolysis at D_{144}-I_{145} resulting in loss of a single amino acid residue in such a flexible region is also not

likely to impact protein stability. Similar effects were also observed for the N-terminal flexible extensions of IAAB and IAAD (Fig. S1D, S2E).

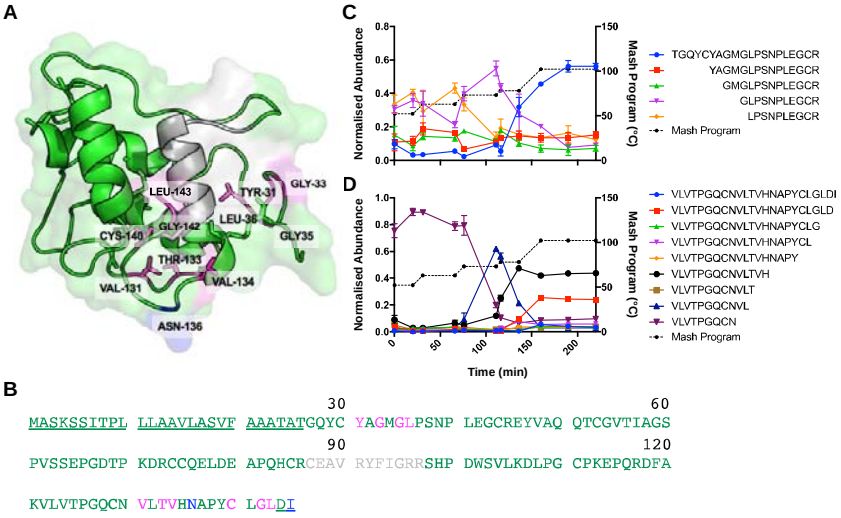

Figure 5. Select sites of proteolysis do not affect IAAA stability. (A) Cartoon of the X-ray crystal structure of IAAA, homology modelled on 1B1U (38). Green, peptides identified by MS; grey, unidentified peptides; magenta and labelled, amino acid after a proteolytic cleavage event; blue and labelled, amino acid after a proteolytic cleavage event that does not lower stability. **(B)** IAAA protein sequence with the same colour scheme as (A). Underlined, not present in structure. Normalised abundance (a.u; arbitrary units) of full- and semi-tryptic peptides corresponding to **(C)** T_{26}GQYCYAGMGLPSNPLEGCR$_{45}$-E and **(D)** K-V_{122}LVTPGQCNVLTVHNAPYCLGLDI$_{145}$. Values show mean, n=3. Error bars show SD. Mash temperature profile is shown on the right Y-axis. Mash program is shown in black dotted lines; points indicate when samples were taken.

In summary, our data showed that extensive proteolysis during the early stages of the mash lowers the unfolding temperature of diverse proteins and explains why a large fraction of each protein unfolds, aggregates, and is lost from solution at higher temperatures. Those proteins which escape proteolysis, or which are clipped at specific sites that do not affect thermal stability, remain present even after the boil, explaining the sustained presence of a fraction of each protein through the boil and potentially into beer.

In addition to proteolysis, we also identified modification of diverse proteins by oxidation, glycation, and deamidation. Oxidation has been reported on selected proteins in beer and found to decrease as temperature increased (35). Glycation is driven by the Maillard reaction, where reducing sugars modify primarily lysine residues, catalysed by high temperature (12, 32, 39). The mash and boil therefore provide a perfect environment for glycation to take place. Although we could identify diverse sites of these modifications, data quality was insufficient to quantitatively monitor their abundance throughout the mash.

Discussion

We used SWATH-MS to investigate the changes in the wort proteome throughout the mash and boil stages of beer brewing. Our results showed that the mash proteome was highly dynamic, with proteins increasing in abundance as they were extracted from the malt early in the mash, and then rapidly decreasing in abundance at higher temperatures due to thermal denaturation, aggregation, and precipitation.

Correlation profiling of protein abundance throughout the mash identified four clusters of proteins with distinct temperature-dependent abundance profiles and distinct physiochemical properties (Fig. 3). Each of these clusters were defined by the presence of multiple protein homologs with similar sequence and structure. Our data showed that these sequence characteristics were clearly critical in determining protein abundance through the mash and into beer. However, it is likely that other process parameters such as altered germination extent during malting, grist particle size from differential grinding, or extraction efficiency through varied grist:liquor ratios would also have substantial effects on protein abundance profiles

The proteome of the soluble wort throughout the mash and boil was extremely complex, with many proteins undergoing diverse modifications. Many of these modifications functionally affected protein stability and thus abundance within the wort over the temperature profile of the mash and boil. We identified abundant proteolysis during the early stages of the mash, and correlated proteolysis with low thermal stability and specific loss of clipped proteins from the wort at higher temperatures. Extensive proteolysis and subsequent thermal destabilisation explained

why a large fraction of each protein was denatured and removed from the soluble wort at higher temperatures. A small fraction of each protein generally remained soluble after the boil, due to a lack of proteolysis or only being clipped at specific sites that did not perturb thermal stability.

The proteome of the wort during the mash and boil is highly complex. Protein abundance during the mash is reliant on chemical and biophysical processes including solubilisation, proteolysis, oxidation, glycation, unfolding, and aggregation. Protein structure and stability determines whether a protein survives intact throughout the mash and boil to be present in the final soluble wort, and protein structure and stability is in turn directly affected by modifications, primarily proteolysis. Our data showed that extensive proteolytic cleavage explained why a large percentage of proteins were lost from the soluble wort during the mash and boil. Generally, proteolysis caused structural instability at high temperatures, leading to unfolding, aggregation, and precipitation (Fig. 4, 5, Fig. S1 – S3). However, a few specific proteolytic events did not affect protein stability. These were present in unstructured terminal regions of proteins, or close to networks of disulphide bonds that would be expected to lock the local protein fold. These specific events left the proteins with sufficient stability to survive the boil intact. Interestingly, our data showed no correlation between the extent or ease of proteolysis and the subsequent impact of specific proteolytic events on protein stability. This suggests that the extent of proteolysis and the likelihood of subsequent protein unfolding are largely independent. Proteolysis is likely driven by substrate accessibility and the presence of specific recognition motifs, while unfolding of proteolytically clipped proteins is less predictable and highly dependent on local protein context.

A critical concern of the brewing industry is efficient digestion of starch to oligomaltose, which requires maintaining high activity of both α- and β-amylase throughout the mash. α-Amylase cleaves internal α(1-4) glucosidic bonds in starch, while β-amylase releases maltose disaccharides from the non-reducing ends of starch polymers or maltooligosaccharides (1, 3, 23). Maintaining high α- and β-amylase activity is made difficult by the low unfolding temperature of β-amylase relative to α-amylase (3, 24, 25). It is generally accepted that a mash temperature of ~65°C is

appropriate to keep both enzymes stable while allowing efficient conversion of starch to oligomaltose, but high enough to allow adequate gelatinization of starch (1, 3). Our results confirmed that a mash temperature of ~65°C is appropriate for these aims, as both α- and β-amylase were stable at the 63˚C maltose rest (Fig. 2C). Another key concern in industrial brewing is production of sufficient FAN to ensure robust yeast growth during fermentation. Our data demonstrated that proteolysis was extensive at lower temperatures (Fig. 4, 5, Fig. S1 – S3). Use of a mash profile with a low temperature stage such as a protein rest at 53˚C is therefore required to achieve high FAN. However, our data also clearly demonstrated the challenges in balancing adequate FAN production with efficient starch degradation, as increased proteolysis would result in more proteolytically clipped α- and β-amylase with reduced enzymatic activity and lower thermostability. The dynamic brewing proteome and metabolome are therefore highly dependent on the abundance and structure of the starch, enzymes, and other proteins in the malt; the precise mash profile used; and the complex interplay between protein post-translational modification, activity, and stability.

Proteomics can measure aspects of the complex protein biochemistry of beer brewing inaccessible to other methods. Similar analyses could therefore be used to optimize mashing profiles for specific barley varieties, brewery processes, or beer styles based on the abundance of amylases, proteases, and other proteins. Our data also suggest that proteomics could be used for quality control of barley and malt, and to monitor process efficiency and product quality in other food bioprocessing industries.

References

1. Stewart, G. G. (2013) Biochemistry of Brewing. *Biochemistry of Foods*, Academic Press, San Diego
2. Stewart, G. G., and Priest, F. G. (2006) *Handbook of brewing*, CRC Press
3. Barth, R. (2013) *The Chemistry of Beer: The Science in the Suds*, John Wiley & Sons
4. Iimure, T., Nankaku, N., Kihara, M., Yamada, S., and Sato, K. (2012) Proteome analysis of the wort boiling process. *Food Research International* 45, 262-271
5. Perrocheau, L., Rogniaux, H., Boivin, P., and Marion, D. (2005) Probing heat-stable water-soluble proteins from barley to malt and beer. *Proteomics* 5, 2849-2858
6. Fasoli, E., Aldini, G., Regazzoni, L., Kravchuk, A. V., Citterio, A., and Righetti, P. G. (2010) Les Maitres de l'Orge: the proteome content of your beer mug. *Journal of Proteome Research* 9, 5262-5269
7. Berner, T. S., Jacobsen, S., and Arneborg, N. (2013) The impact of different ale brewer's yeast strains on the proteome of immature beer. *BMC Microbiology* 13, 215
8. Schulz, B. L., Phung, T. K., Bruschi, M., Janusz, A., Stewart, J., Meehan, J., Healy, P., Nouwens, A. S., Fox, G. P., and Vickers, C. E. (2018) Process Proteomics of Beer Reveals a Dynamic Proteome with Extensive Modifications. *Journal of Proteome Research* 17, 1647-1653
9. Colgrave, M. L., Goswami, H., Howitt, C. A., and Tanner, G. J. (2012) What is in a beer? Proteomic characterization and relative quantification of hordein (gluten) in beer. *Journal of Proteome Research* 11, 386-396
10. Picariello, G., Mamone, G., Cutignano, A., Fontana, A., Zurlo, L., Addeo, F., and Ferranti, P. (2015) Proteomics, Peptidomics, and Immunogenic Potential of Wheat Beer (Weissbier). *Journal of Agricultural and Food Chemistry* 63, 3579-3586
11. Van Nierop, S. N. E., Evans, D. E., Axcell, B. C., Cantrell, I. C., and Rautenbach, M. (2004) Impact of Different Wort Boiling Temperatures on the Beer Foam Stabilizing Properties of Lipid Transfer Protein 1. *Journal of Agricultural and Food Chemistry* 52, 3120-3129
12. Jégou, S., Douliez, J.-P., Mollé, D., Boivin, P., and Marion, D. (2001) Evidence of the glycation and denaturation of LTP1 during the malting and brewing process. *Journal of Agricultural and Food Chemistry* 49, 4942-4949
13. Savitski, M. M., Reinhard, F. B., Franken, H., Werner, T., Savitski, M. F., Eberhard, D., Martinez Molina, D., Jafari, R., Dovega, R. B., Klaeger, S., Kuster, B., Nordlund, P., Bantscheff, M., and Drewes, G. (2014) Tracking cancer drugs in living cells by thermal profiling of the proteome. *Science* 346, 1255784
14. Mateus, A., Määttä, T. A., and Savitski, M. M. (2017) Thermal proteome profiling: Unbiased assessment of protein state through heat-induced stability changes. *Proteome Science* 15, 1-7
15. Huber, K. V. M., Olek, K. M., Müller, A. C., Soon, C., Tan, H., and Keiryn, L. (2015) Proteome-wide small molecule and metabolite interaction mapping. *Nature methods* 12, 1055-1057
16. Becher, I., Werner, T., Doce, C., Zaal, E. A., Tögel, I., Khan, C. A., Rueger, A., Muelbaier, M., Salzer, E., Berkers, C. R., Fitzpatrick, P. F., Bantscheff, M., and Savitski, M. M. (2016) Thermal profiling reveals phenylalanine hydroxylase as an off-target of panobinostat. *Nature Chemical Biology* 12, 908-910

17. Xu, Y., Bailey, U. M., and Schulz, B. L. (2015) Automated measurement of site-specific N-glycosylation occupancy with SWATH-MS. *Proteomics* 15, 2177-2186
18. Zacchi, L. F., and Schulz, B. L. (2016) SWATH-MS glycoproteomics reveals consequences of defects in the glycosylation machinery. *Molecular & Cellular Proteomics* 15, 2435-2447
19. Vizcaíno, J. A., Csordas, A., Del-Toro, N., Dianes, J. A., Griss, J., Lavidas, I., Mayer, G., Perez-Riverol, Y., Reisinger, F., Ternent, T., Xu, Q.-W., Wang, R., and Hermjakob, H. (2016) 2016 update of the PRIDE database and its related tools. *Nucleic Acids Research* 44, D447-D456
20. de Hoon, M. J. L., Imoto, S., Nolan, J., and Miyano, S. (2004) Open source clustering software. *Bioinformatics* 20, 1453-1454
21. Osorio, D., Rondon-Villarreal, P., and Torres, R. (2015) Peptides: A Package for Data Mining of Antimicrobial Peptides. *The R Journal* 7, 4-14
22. Falcon, S., and Gentleman, R. (2007) Using GOstats to test gene lists for GO term association. *Bioinformatics* 23, 257-258
23. Briggs, D. E., Boulton, C. A., Brookes, P. A., and Stevens, R. (2004) *Brewing Science and Practice*, Woodhead Publishing
24. Hu, S., Dong, J., Fan, W., Yu, J., Yin, H., Huang, S., Liu, J., Huang, S., and Zhang, X. (2014) The influence of proteolytic and cytolytic enzymes on starch degradation during mashing. *Journal of the Institute of Brewing* 120, 379-384
25. Muller, R. (1991) The effects of mashing temperature and mash thickness on wort carbohydrate composition. *Journal of the Institute of Brewing* 97, 85-92
26. Evans, D. E., and Hejgaard, J. (1999) The impact of malt derived proteins on beer foam quality. Part I. The effect of germination and kilning on the level of protein Z4, protein Z7 and LTP1. *Journal of the Institute of Brewing* 105, 159-170
27. Evans, D. E., Sheehan, M., and Stewart, D. (1999) The Impact of Malt Derived Proteins on Beer Foam Quality. Part II: The Influence of Malt Foam‐positive Proteins and Non‐starch Polysaccharides on Beer Foam Quality. *Journal of the Institute of Brewing* 105, 171-178
28. Hao, J., Dong, J., Yu, J., Gu, G., Chen, J., Li, Q., and Fan, W. (2006) Identification of the major proteins in beer foam by mass spectrometry following sodium dodecyl sulfate-polyacrylamide gel electrophoresis. *Journal of the American Society of Brewing Chemists* 64, 166-174
29. Østergaard, O., Finnie, C., Laugesen, S., Roepstorff, P., and Svennson, B. (2004) Proteome analysis of barley seeds: Identification of major proteins from two-dimensional gels (pI 4-7). *Proteomics* 4, 2437-2447
30. Østergaard, O., Melchior, S., Roepstorff, P., and Svensson, B. (2002) Initial proteome analysis of mature barley seeds and malt. *Proteomics* 2, 733-739
31. Grochalová, M., Konečná, H., Stejskal, K., Potěšil, D., Fridrichová, D., Srbová, E., Ornerová, K., and Zdráhal, Z. (2017) Deep coverage of the beer proteome. *Journal of Proteomics* 162, 119-124
32. Petry-Podgorska, I., Zidkova, J., Flodrova, D., and Bobalova, J. (2010) 2D-HPLC and MALDI-TOF/TOF analysis of barley proteins glycated during brewing. *Journal of Chromatography B* 878, 3143-3148
33. Taylor, J., and Boyd, H. K. (1986) Free α‐amino nitrogen production in sorghum beer mashing. *Journal of the Science of Food and Agriculture* 37, 1109-1117
34. Mikola, J., Pietilå, K., and Enari, T. M. (1972) Inactivation of malt peptidases during mashing. *Journal of the Institute of Brewing* 78, 384-388

35. Pöyri, S., Mikola, M., Sontag‐Strohm, T., Kaukovirta‐Norja, A., and Home, S. (2002) The Formation and Hydrolysis of Barley Malt Gel‐Protein Under Different Mashing Conditions. *Journal of the Institute of Brewing* 108, 261-267
36. Rübsam, H., Gastl, M., and Becker, T. (2013) Determination of the influence of starch sources and mashing procedures on the range of the molecular weight distribution of beer using field-flow fractionation. *Journal of the Institute of Brewing* 119, 139-148
37. Bering, C. L. (1988) The Biochemistry of Brewing. *Journal of Chemical Education* 65, 519-521
38. Gourinath, S., Alam, N., Srinivasan, A., Betzel, C., and Singh, T. P. (2000) Structure of the bifunctional inhibitor of trypsin and alpha-amylase from ragi seeds at 2.2 A resolution. *Acta Crystallogr D Biol Crystallogr* 56, 287-293
39. Martins, S. I., Jongen, W. M., and Van Boekel, M. A. (2000) A review of Maillard reaction in food and implications to kinetic modelling. *Trends in Food Science & Technology* 11, 364-373
40. Ludvigsen, S., and Poulsen, F. M. (1992) Three-dimensional structure in solution of barwin, a protein from barley seed. *Biochemistry* 31, 8783-8789

Acknowledgements

We gratefully acknowledge the assistance of Dr Amanda Nouwens and Mr Peter Josh at The University of Queensland School of Chemistry and Molecular Biosciences Mass Spectrometry Facility.

Supplementary Material

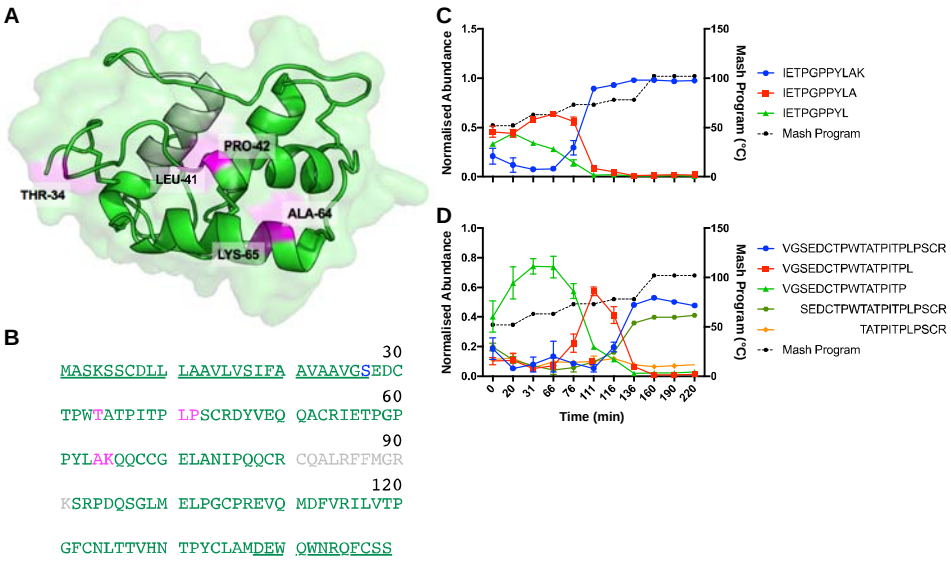

Supplementary Figure 1. Select sites of proteolysis do not affect IAAB stability. **(A)** Cartoon of the X-ray crystal structure of IAAB, homology modelled on 1B1U (38). Green, peptides identified by MS; grey, unidentified peptides; magenta and labelled, amino acid after a proteolytic cleavage event. **(B)** IAAB protein sequence with the same colour scheme as (A). Underlined, not present in structure; blue, amino acid after a proteolytic cleavage event that does not lower stability. Normalised abundance (a.u; arbitrary units) of full- and semi-tryptic peptides corresponding to **(C)** R-I_{55}ETPGPPYLAK_{65}-Q and **(D)** V-$_{25}$GSEDCTPWTATPITPLPSCR_{45}-D. Values show mean, n=3. Error bars show SD. Mash temperature profile is shown on the right Y-axis. Mash program is shown in black dotted lines; points indicate when samples were taken.

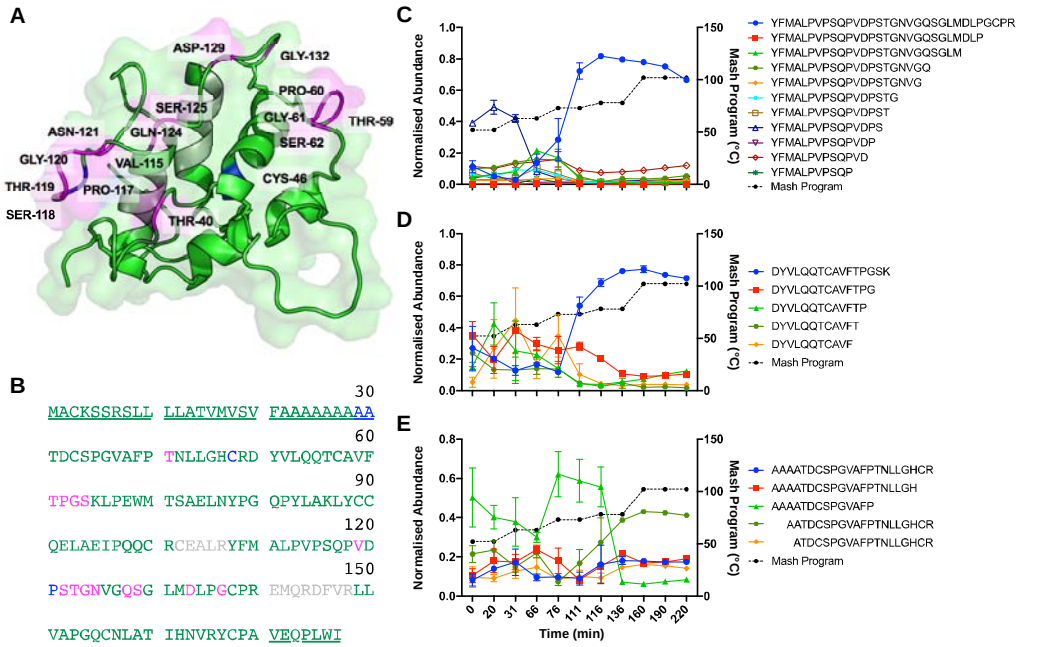

Supplementary Figure 2. Select sites of proteolysis do not affect IAAD stability. **(A)** Cartoon of the X-ray crystal structure of IAAD, homology modelled on 1B1U (38). Green, peptides identified by MS; grey, unidentified peptides; magenta and labelled, amino acid after a proteolytic cleavage event. **(B)** IAAD protein sequence with the same colour scheme as (A). Underlined, not present in structure; blue, amino acid after a proteolytic cleavage event that does not lower stability. Normalised abundance (a.u; arbitrary units) of full- and semi-tryptic peptides corresponding to **(C)** R-Y_{104}FMALPVPSQPVDPSTGNVGQSGLMDLPGCPR$_{135}$-E, **(D)** D_{48}YVLQQTCAVFTPGSK$_{63}$-L, and **(E)** A_{25}AAATDCSPGVAFPTNLLGHCR$_{47}$-D. Values show mean, n=3. Error bars show SD. Mash temperature profile is shown on the right Y-axis. Mash program is shown in black dotted lines; points indicate when samples were taken.

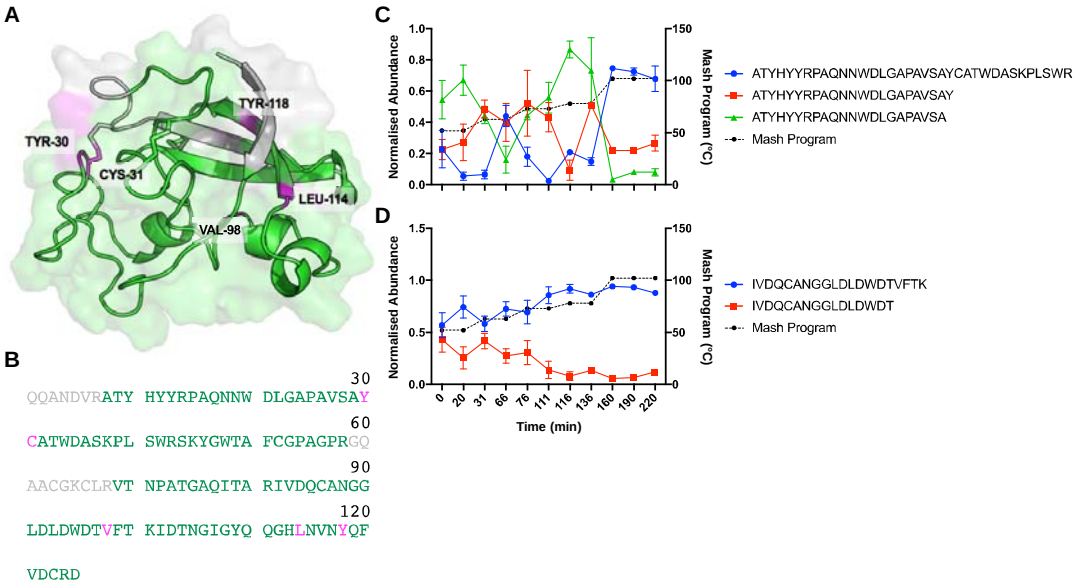

Supplementary Figure 3. Proteolysis during the mash lowers the stability of BARW. (A) Cartoon of the X-ray crystal structure of BARW (1BW3) (40). Green, peptides identified by MS; grey, unidentified peptides; magenta and labelled, amino acid after a proteolytic cleavage event. **(B)** BARW protein sequence with the same colour scheme as (A). Underlined, not present in structure. Normalised abundance (a.u; arbitrary units) of full- and semi-tryptic peptides corresponding to **(C)** R-A_8TYHYYRPAQNNWDLGAPAVSAYCATWDASKPLSWR$_{43}$-S and **(D)** R-I_{82}VDQCANGGLDLDWDTVFTK$_{101}$-I. Values show mean, n=3. Error bars show SD. Mash temperature profile is shown on the right Y-axis. Mash program is shown in black dotted lines; points indicate when samples were taken.

Supplementary Table 1. Temperature stages used in the mash.

Stage	Temperature (°C)	Length of stage (min)
Protein rest	52°C	20 min
Maltose rest	63°C	35 min
Sugar rest 1	73°C	35 min
Sugar rest 2	78°C	20 min
Boil	102°C	60 min

Supplementary Table 2. GO term enrichment for the four protein clusters identified by correlation profiling of protein abundance throughout the mash. Ontology indicates the type of GO term: biological process (BP), molecular function (MF), or chemical component (CC). All GO terms shown were considered significant ($p < 0.05$). GO term enrichment was performed with GOstats.

GO ID	Ontology	P value	Term	Gene IDs
Cluster 1				
GO:0008289	MF	0.003	lipid binding	NLTP1_HORVU;NLTP2_HORVU;NLTP3_LENCU;NLTP3_WHEAT
GO:0010876	BP	0.031	lipid localization	NLTP1_HORVU;NLTP3_LENCU;NLTP3_WHEAT
GO:0006869	BP	0.031	lipid transport	NLTP1_HORVU;NLTP3_LENCU;NLTP3_WHEAT
GO:0006810	BP	0.036	transport	NLTP1_HORVU;NLTP2_HORVU;NLTP3_LENCU;NLTP3_WHEAT
GO:0051234	BP	0.036	establishment of localization	NLTP1_HORVU;NLTP2_HORVU;NLTP3_LENCU;NLTP3_WHEAT
GO:0051179	BP	0.036	localization	NLTP1_HORVU;NLTP2_HORVU;NLTP3_LENCU;NLTP3_WHEAT
GO:0044092	BP	0.046	negative regulation of molecular function	IAA1_HORVU;IAAE_HORVU
GO:0043086	BP	0.046	negative regulation of catalytic activity	IAA1_HORVU;IAAE_HORVU
Cluster 2				
GO:0030234	MF	0.001	enzyme regulator activity	BSZ7_HORVU;CYT4_ORYSJ;HINB2_HORVU;IAA2_HORVU;IAAA_HORVU;IAAB_HORVU;IAAD_HORVU;IAA_HORVU;IAC16_WHEAT;ICIA_HORVU;ICIB_HORVU
GO:0098772	MF	0.001	molecular function regulator	BSZ7_HORVU;CYT4_ORYSJ;HINB2_HORVU;IAA2_HORVU;IAAA_HORVU;IAAB_HORVU;IAAD_HORVU;IAA_HORVU;IAC16_WHEAT;ICIA_HORVU;ICIB_HORVU
GO:0004866	MF	0.001	endopeptidase inhibitor activity	BSZ7_HORVU;CYT4_ORYSJ;HINB2_HORVU;IAA2_HORVU;IAAA_HORVU;IAAB_HORVU;IAAD_HORVU;IAA_HORVU;IAC16_WHEAT;ICIA_HORVU;ICIB_HORVU
GO:0004857	MF	0.001	enzyme inhibitor activity	BSZ7_HORVU;CYT4_ORYSJ;HINB2_HORVU;IAA2_HORVU;IAAA_HORVU;IAAB_HORVU;IAAD_HORVU;IAA_HORVU;IAC16_WHEAT;ICIA_HORVU;ICIB_HORVU
GO:0030414	MF	0.001	peptidase inhibitor activity	BSZ7_HORVU;CYT4_ORYSJ;HINB2_HORVU;IAA2_HORVU;IAAA_HORVU;IAAB_HORVU;IAAD_HORVU;IAA_HORVU;IAC16_WHEAT;ICIA_HORVU;ICIB_HORVU
GO:0061134	MF	0.001	peptidase regulator activity	BSZ7_HORVU;CYT4_ORYSJ;HINB2_HORVU;IAA2_HORVU;IAAA_HORVU;IAAB_HORVU;IAAD_HORVU;IAA_HORVU;IAC16_WHEAT;ICIA_HORVU;ICIB_HORVU
GO:0061135	MF	0.001	endopeptidase regulator activity	BSZ7_HORVU;HINB2_HORVU;IAA2_HORVU;IAAA_HORVU;IAAB_HORVU;IAAD_HORVU;IAA_HORVU;IAC16_WHEAT;ICIA_HORVU;ICIB_HORVU
GO:0004867	MF	0.003	serine-type endopeptidase inhibitor activity	IAA2_HORVU;IAAA_HORVU;IAAB_HORVU;IAAD_HORVU;IAA_HORVU;IAC16_WHEAT
GO:0015066	MF	0.013	alpha-amylase inhibitor activity	ALF2_CAEEL;NDK1_SACOF;NRDR3_MAGSA;TPIS_HORVU
GO:0006139	BP	0.049	nucleobase-containing compound metabolic process	
Cluster 3				
GO:0016798	MF	0.000	hydrolase activity, acting on glycosyl bonds	AMY2_HORVU;AMY4_CAPCH;AMY6_HORVU;AMYB_HORVS;AMYB_HORVU;BGL26_ORYSJ;CHI1_HORVU;CHI2_HORVU
GO:0004553	MF	0.000	hydrolase activity, hydrolyzing O-glycosyl compounds	AMY2_HORVU;AMY4_CAPCH;AMY6_HORVU;AMYB_HORVS;AMYB_HORVU;BGL26_ORYSJ;CHI1_HORVU;CHI2_HORVU
GO:0016787	MF	0.000	hydrolase activity	AMY2_HORVU;AMY4_CAPCH;AMY6_HORVU;AMYB_HORVS;AMYB_HORVU;BGL26_ORYSJ;CHI1_HORVU;CHI2_HORVU;CTPC_MYCLE
GO:0003824	MF	0.000	catalytic activity	AMY2_HORVU;AMY4_CAPCH;AMY6_HORVU;AMYB_HORVS;AMYB_HORVU;BGL26_ORYSJ;CHI1_HORVU;CHI2_HORVU;CTPC_MYCLE;GRDH_ORYSJ;LGUL_ORYSJ;NUON_AERHH
GO:0016160	MF	0.001	amylase activity	AMY2_HORVU;AMY4_CAPCH;AMY6_HORVU;AMYB_HORVS;AMYB_HORVU

GO:0004556	MF	0.019	alpha-amylase activity	AMY2_HORVU;AMY4_CAPCH;AMY6_HORVU
GO:0004568	MF	0.032	chitinase activity	CHI1_HORVU;CHI2_HORVU
GO:0016161	MF	0.032	beta-amylase activity	AMYB_HORVS;AMYB_HORVU
GO:0005975	BP	0.000	carbohydrate metabolic process	AMY2_HORVU;AMY4_CAPCH;AMY6_HORVU;AMYB_HORVS;AMYB_HORVU;BGL26_ORYSJ;CHI1_HORVU;CHI2_HORVU
GO:0071704	BP	0.000	organic substance metabolic process	AMY2_HORVU;AMY4_CAPCH;AMY6_HORVU;AMYB_HORVS;AMYB_HORVU;BGL26_ORYSJ;CHI1_HORVU;CHI2_HORVU;NUON_AERHH
GO:0044238	BP	0.000	primary metabolic process	AMY2_HORVU;AMY4_CAPCH;AMY6_HORVU;AMYB_HORVS;AMYB_HORVU;BGL26_ORYSJ;CHI1_HORVU;CHI2_HORVU;NUON_AERHH
GO:0009057	BP	0.000	macromolecule catabolic process	AMYB_HORVS;AMYB_HORVU;CHI1_HORVU;CHI2_HORVU
GO:0000272	BP	0.000	polysaccharide catabolic process	AMYB_HORVS;AMYB_HORVU;CHI1_HORVU;CHI2_HORVU
GO:0008152	BP	0.001	metabolic process	AMY2_HORVU;AMY4_CAPCH;AMY6_HORVU;AMYB_HORVS;AMYB_HORVU;BGL26_ORYSJ;CHI1_HORVU;CHI2_HORVU;NUON_AERHH
GO:0005976	BP	0.002	polysaccharide metabolic process	AMYB_HORVS;AMYB_HORVU;CHI1_HORVU;CHI2_HORVU
GO:0016052	BP	0.020	carbohydrate catabolic process	AMYB_HORVS;AMYB_HORVU;CHI1_HORVU;CHI2_HORVU
GO:0006022	BP	0.025	aminoglycan metabolic process	CHI1_HORVU;CHI2_HORVU
GO:0006026	BP	0.025	aminoglycan catabolic process	CHI1_HORVU;CHI2_HORVU
GO:0006040	BP	0.025	amino sugar metabolic process	CHI1_HORVU;CHI2_HORVU
GO:0006030	BP	0.025	chitin metabolic process	CHI1_HORVU;CHI2_HORVU
GO:0006032	BP	0.025	chitin catabolic process	CHI1_HORVU;CHI2_HORVU
GO:0016998	BP	0.025	cell wall macromolecule catabolic process	CHI1_HORVU;CHI2_HORVU
GO:0071554	BP	0.025	cell wall organization or biogenesis	CHI1_HORVU;CHI2_HORVU
GO:0046348	BP	0.025	amino sugar catabolic process	CHI1_HORVU;CHI2_HORVU
GO:0044036	BP	0.025	cell wall macromolecule metabolic process	CHI1_HORVU;CHI2_HORVU
GO:1901136	BP	0.025	carbohydrate derivative catabolic process	CHI1_HORVU;CHI2_HORVU
GO:1901071	BP	0.025	glucosamine-containing compound metabolic process	CHI1_HORVU;CHI2_HORVU
GO:1901072	BP	0.025	glucosamine-containing compound catabolic process	CHI1_HORVU;CHI2_HORVU
GO:1901575	BP	0.033	organic substance catabolic process	AMYB_HORVS;AMYB_HORVU;CHI1_HORVU;CHI2_HORVU
GO:0009056	BP	0.033	catabolic process	AMYB_HORVS;AMYB_HORVU;CHI1_HORVU;CHI2_HORVU
GO:0044425	CC	0.004	membrane part	CTPC_MYCLE;NUON_AERHH
GO:0031224	CC	0.004	intrinsic component of membrane	CTPC_MYCLE;NUON_AERHH
GO:0016021	CC	0.004	integral component of membrane	CTPC_MYCLE;NUON_AERHH
GO:0071944	CC	0.007	cell periphery	CTPC_MYCLE;NUON_AERHH
GO:0005886	CC	0.007	plasma membrane	CTPC_MYCLE;NUON_AERHH
GO:0016020	CC	0.033	membrane	CTPC_MYCLE;NUON_AERHH
Cluster 4				
GO:0003824	MF	0.032	catalytic activity	AMY1_HORVU;CYSP2_HORVU;G3PC1_HORVU;HIS6_CHLT3;PDI_WHEAT;PIMT_METMJ;REHY_HORVU;SODC2_ORYSJ
GO:0044267	BP	0.023	cellular protein metabolic process	PIMT_METMJ;RS142_MAIZE;RUB1_ARATH
GO:0005737	CC	0.048	cytoplasm	G3PC1_HORVU;HIS6_CHLT3;PDI_WHEAT;PIMT_METMJ;RS142_MAIZE;RUB1_ARATH;SODC2_ORYSJ

[1] Biological Process
[2] Molecular Function
[3] Cellular Compartment